The Galactic Population of Post-Asymptotic Giant Branch Stars: First Distance Catalogue

MACQUARIE UNIVERSITY

David J. Frew[1], Shane B. Vickers[1], Quentin A. Parker[1,2] and Ivan S. Bojicic[1,2]

AAO

[1] Department of Physics and Astronomy, Macquarie University, Sydney, NSW [2] Australian Astronomical Observatory, Epping, NSW

Introduction

We have commenced a detailed analysis of the known sample of Galactic post-asymptotic giant branch (PAGB) objects compiled in the Toruń Catalogue of Szczerba et al. (2007, 2012), and present, for the first time, homogeneously derived distance determinations for the 209 likely and 87 possible catalogued PAGB stars from that compilation. Knowledge of PAGB distances is essential in determining meaningful physical characteristics for these sources and this has been difficult to determine for most objects previously. The distances were determined by modeling their spectral energy distributions (SEDs) with multiple black-body curves, and integrating under the overall fit to determine the total distance-dependent flux.

We have used a standard-candle luminosity to estimate the SED distances. For Galactic thin disk objects, we use several luminosity bins based on typical observational characteristics, ranging between 3500 and 20000L$_\odot$. We further adopt a default luminosity of 1700 L$_\odot$ for all Population II objects. We have also applied the above technique to a further sample of 80 related nebulae not in the current edition of the Toruń catalogue, some of these being well known PAGB mimics (see Frew & Parker 2010). The full details on our technique, and the catalogue of distances for all 376 objects, are given in Vickers et al. (2013).

Observational Sample

The Toruń catalogue provides easy online access to processed photometric and spectroscopic data for the currently identified Galactic population of PAGB stars and related objects. With the advent of this compilation of all known objects and flux data, our distance technique can be applied to the known PAGB population, leading to a large-enough sample to exploit for scientific purposes. The catalogue is divided into five categories: (i) very-likely PAGB stars, (ii) RV Tauri stars, (iii) R Coronae Borealis / extreme Helium / Late thermal pulse stars, (iv) possible PAGB stars, and (v) unlikely PAGB objects. In our first paper, we mostly restrict our analysis to the first two categories.

Supplementary Data

We have also utilised a number of additional sources that supplement the flux data presented in the Toruń catalogue. These include fluxes from several minor surveys, plus data that has been published since the most recent release of the catalogue (v2.0; Szczerba et al. 2007, 2012). To gather much of these data, we interrogated the fifth edition of the Catalogue of Infrared Observations (Gezari, Pitts & Schmitz 1999, and references therein). This is a valuable source of literature data, but the catalogue includes both line and continuum fluxes, and data obtained using different aperture diameters, so in order to remove problematic fluxes we needed to carefully vet the data, object by object. To do this we used the new online Macquarie database, detailed by Parker et al. (2013) at this meeting. We also used more recent mid-IR flux data from the literature for individual sources if available. Table 1 gives a comparison of the wavelengths and the angular resolution of each data set that was utilised.

Table 1: Supplementary data to the Torun catalogue used to make the SED fits.

Survey/Catalogue	Wavebands ($\lambda_{\rm eff}$ μm)	Resolution
TD-1	0.157, 0.197, 0.237, 0.274	$\sim7'$
ANS	0.155, 0.180, 0.220, 0.250, 0.330	$2.5'$
GALEX	FUV (0.44), NUV (0.51)	~4–$6''$
Tycho-2	B_T (0.44), V_T (0.51)	$\sim0.8''$
DENIS	I (0.82), J (1.25), K_s (2.15)	1–$3''$
2MASS	J (1.24), H (1.66), K_s (2.16)	$2''$
UKIDSS	Z (0.88), Y (1.03), J (1.25), H (1.66), K_s (2.15)	$1''$
WISE	W1 (3.4), W2 (4.6), W3 (12), W4 (22)	6–$12''$
Spitzer (IRAC)	IRAC1 (3.6), IRAC2 (4.5), IRAC3 (5.8), IRAC4 (8.0)	$\leqslant2''$
RAFGL	4.2, 11.0, 19.8, 27.4	$3.5'$
MSX6C	A (8.3), C (12.1), D (14.7), E (21.3)	$18''$
AKARI (IRC)	S9W (9.0), L18W (18.0)	$\sim2''$
AKARI (FIS)	65, 90, 140, 160	30–$50''$
COBE/DIRBE^a	3.5, 4.9, 12, 25, 60	$40'$
IRAS	12, 25, 60, 100	0.5–$2'$
Spitzer (MIPS)	24, 70, 160	$\sim6''$
Herschel (PACS)	blue (70), red (160)	5–$35''$
Herschel (SPIRE)	PSW (250), PMW (350), PLW (500)	5–$35''$
SCUBA	450, 850	8–$14''$
Planck^b	857 GHz (350), 545 GHz (550), 353 GHz (849)	5–$30'$

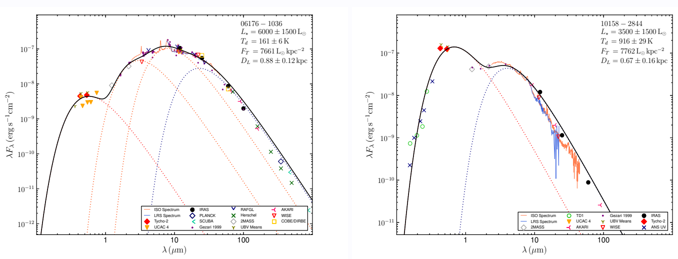

Figure 1: Representative SEDs for two post-AGB objects: the Red Rectangle (left) and HR 4049 (right).

Method

The SED method works because the luminosity of these central stars is very nearly constant from the tip of the AGB phase to the beginning of the white-dwarf cooling track (Schoenberner 1983; Vassiliadis & Wood 1994). This then enables us to use a standard-candle luminosity to estimate the SED distances. For Galactic thin-disk objects, we use several luminosity bins based on typical observational characteristics, ranging between 3500 and 20,000 L$_\odot$. We further adopt a default luminosity of 1700 L$_\odot$ for all Population II objects. We have also applied the above technique to a further sample of 80 related nebulae not in the current edition of the Toruń catalogue.

From the fitting process we were able to derive a number of parameters for each object. The total monochromatic flux (in units of L$_\odot$ kpc^{-2}) was derived via numerical integration of the superposition of the Planck functions, integrated from 1000 Å to infinity. The luminosity dependent distance is then simply:

$$D^2 = L_\star / 4\pi F$$

where $L_\star$ is the assumed stellar luminosity (in solar units) and F is the integrated flux expressed in L$_\odot$ kpc^{-2}. For most disk objects, we use L$_\star$ = 6000 L$_\odot$, while for low-mass Galactic thick disk objects and metal-poor Population II stars the assumed luminosity becomes 1700 − 2000 L$_\odot$ as discussed by Vickers et al. (2013). The distance uncertainty is derived from the quadratic sum of the uncertainties in the fluxes, the overall fit, and the assumed luminosity.

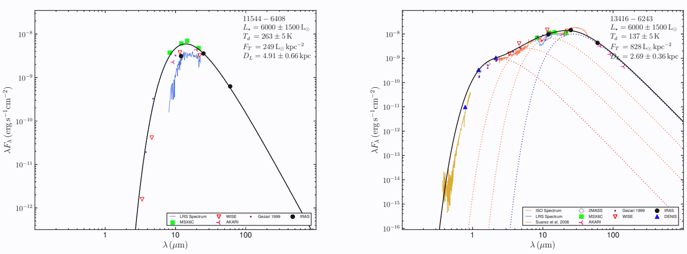

Figure 2 (above): SEDs for two more objects: GLMP 315 (left) and IRAS 13416-6243 (right).

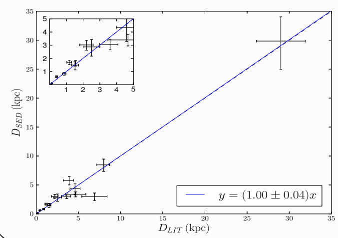

Figure 3 (left): A comparison of our SED fitting distances with reliable independent distances taken from the literature for 20 post-AGB stars, dusty AGB stars and young, compact PNe. These distances are measured using several primary techniques, such as trigonometric parallaxes, expansion parallaxes, or phase-lag measurements. A least squares fit of the data has a slope of 1.00 ± 0.04 indicating that the two data sets are in very good agreement. Thus, our SED technique is robust, provided the best quality data are used to make the fits.

Distance Catalogue

Table 2, below, shows a ten-line extract from the catalogue presented in Vickers et al. (2013). The column headings are self-explanatory, and the last two columns show the estimated blackbody temperature of the coolest dust component and the ratio of the flux of this component to the stellar luminosity.

IRAS No.	Other Name	l (°)	b (°)	Flux (erg s^{-1} cm^{-2})	Flux (L$_\odot$ kpc^{-2})	Luminosity (L$_\odot$)	Distance (kpc)	T_d (K)	$F_{\rm IR}/F_\star$
17581−2926	GLMP 688	1.293	−3.199	1.34E-09	42	3500 ± 1500	9.16 ± 2.24	111 ± 27	2.85
17291−2402	GLMP 575	2.518	5.120	4.11E-09	128	3500 ± 1500	5.23 ± 1.28	126 ± 4	37
17349−2444	GLMP 593	2.652	3.637	2.27E-09	70	3500 ± 1500	7.05 ± 1.72	113 ± 3	16
18371−3159	LSE 63	2.918	−11.818	1.47E-09	46	6000 ± 1500	11.44 ± 1.53	134 ± 5	2.07
17576−2653	…	3.472	−1.853	3.29E-09	102	3500 ± 1500	5.85 ± 1.43	121 ± 2	5.72
17516−2525	GLMP 662	4.038	0.056	5.01E-08	1559	6000 ± 1500	1.96 ± 0.26	125 ± 11	1.10
17074−1845	LSE 3	4.100	12.263	2.50E-09	78	6000 ± 1500	8.78 ± 1.18	144 ± 1	3.28
17441−2411	Silkworm Nebula	4.223	2.145	3.14E-08	977	9000 ± 3000	3.03 ± 0.56	119 ± 5	115
17332−2215	GLMP 588	4.542	5.295	2.64E-09	82	3500 ± 1500	6.53 ± 1.59	129 ± 5	20
17360−2142	GLMP 600	5.364	5.038	2.29E-09	71	3500 ± 1500	7.01 ± 1.71	125 ± 6	7.25

Summary and Future Work

We have produced the first catalogue of homogeneously derived distances to the population of Galactic PAGB stars. As we have undertaken a statistical approach, we made the simplifying assumption of fitting blackbody curves to the SEDs we built for each object. In a follow-up paper we will estimate distances to the RV Tauri variables and R CrB stars, allowing a population comparison of these objects with the other subclasses of PAGB stars, as well as with the population of Galactic PNe (Frew 2008; Frew et al. 2013) for the first time.

References

Frew D.J., 2008, PhD Thesis, Macquarie University
Frew D.J., Parker Q.A., 2010, PASA, 27, 129
Frew D.J. et al., 2013, MNRAS, submitted
Gezari D.Y. et al., 1999, VizieR Data Catalog: II/225
Parker Q.A. et al., 2013, these proceedings
Schoenberner D., 1983, ApJ, 272, 708
Szczerba R. et al., 2007, A&A, 469, 799
Szczerba R. et al., 2012, IAUS, 283, 506
Vassiliadis E., Wood P.R., 1994, ApJS, 92, 125
Vickers S.B. et al., 2013, MNRAS, submitted